

1 **What controls the recent changes in African mineral dust aerosol across the Atlantic?**

2 D. A. Ridley<sup>1</sup>, C. L. Heald<sup>1,2</sup>, J. M. Prospero<sup>3</sup>

3 <sup>1</sup> Department of Civil & Environmental Engineering, Massachusetts Institute of Technology,  
4 Cambridge, MA, USA

5 <sup>2</sup> Department of Earth, Atmospheric and Planetary Sciences, Massachusetts Institute of  
6 Technology, Cambridge, MA, USA

7 <sup>3</sup> Rosenstiel School of Marine and Atmospheric Science, University of Miami, Miami, FL, USA

8

9 **Abstract**

10 Dust from Africa strongly perturbs the radiative balance over the Atlantic, with emissions that  
11 are highly variable from year to year. We show that the aerosol optical depth (AOD) of dust over  
12 the mid-Atlantic observed by the AVHRR satellite has decreased by approximately 10% per  
13 decade from 1982 - 2008. This downward trend persists through both winter and summer close  
14 to source and is also observed in dust surface concentration measurements down-wind in  
15 Barbados during summer. The GEOS-Chem model, driven with MERRA re-analysis meteorology  
16 and using a new dust source activation scheme, reproduces the observed trend and is used to  
17 quantify the factors contributing to this trend and the observed variability from 1982 to 2008.  
18 We find that changes in dustiness over the East mid-Atlantic are almost entirely mediated by a  
19 reduction in surface winds over dust source regions in Africa and are not directly linked with  
20 changes in land-use or vegetation cover. The global mean all-sky direct radiative effect (DRE) of  
21 African dust is  $-0.18 \text{ Wm}^{-2}$  at top of atmosphere, accounting for 46% of the global dust total, with  
22 a regional DRE of  $-7.4 \pm 1.5 \text{ Wm}^{-2}$  at the surface of the mid-Atlantic, varying by over  $6.0 \text{ Wm}^{-2}$   
23 from year to year, with a trend of  $+1.3 \text{ Wm}^{-2}$  per decade. These large inter-annual changes and

24 the downward trend highlight the importance of climate feedbacks on natural aerosol  
25 abundance. Our analysis of the CMIP5 models suggests that the decreases in the indirect  
26 anthropogenic aerosol forcing over the North Atlantic in recent decades may be responsible for  
27 the observed climate-response in African dust, indicating a potential amplification of  
28 anthropogenic aerosol radiative impacts in the Atlantic via natural mineral dust aerosol.

29

### 30 **1. Introduction**

31 Mineral dust aerosol is ubiquitous in the atmosphere and arguably the greatest source of  
32 particulate matter. Africa is responsible for approximately half of the global emissions (Huneeus  
33 et al., 2011) resulting in transport of several hundred teragrams (Tg) of dust across the Atlantic  
34 towards the Americas throughout the year (Ginoux et al., 2004; Kaufman et al., 2005a; Ridley et  
35 al., 2012). This has consequences for air quality downwind (Prospero, 1999; Viana et al., 2002) as  
36 well as the radiative balance over the Atlantic, via scattering and absorption of solar radiation  
37 (and to a lesser extent terrestrial radiation), affecting cloud formation (Kaufman et al., 2005b;  
38 Koren et al., 2010; Twohy et al., 2009) and tropical cyclone formation (Dunion and Velden, 2004;  
39 Evan et al., 2006). African dust emissions vary greatly from year to year (Ben-Ami et al., 2012;  
40 Chiapello, 2005; Ginoux et al., 2004), implying considerable variation in the these impacts on  
41 climate and air quality.

42 Global dust emissions vary dramatically on millennial timescales. Sediment core measurements  
43 show that dust deposition over the Atlantic is a factor of 5 higher in the past 2,000 years than  
44 during the African Humid Period (11,700 – 5,000 years ago) and that emissions during glacial  
45 periods are generally 2 - 4 times greater than interglacial periods, likely owing to stronger winds

46 (McGee et al., 2010, 2013). More recently, (Mulitza et al., 2010) determined that dust emissions  
47 from Africa were negatively correlated with tropical West African precipitation from 1000 B.C.  
48 until the end of the 17<sup>th</sup> century but a sharp increase in dust deposition is observed with the  
49 advent of commercial agriculture in the 1800s, indicating the potential for anthropogenic  
50 changes to influence dust emission. Considerable population growth in Africa over recent  
51 decades, by a factor of 3 since 1950 (Prospero and Lamb, 2003), has led to an increase in  
52 agricultural activity and urbanization, with speculation that these human-induced land use and  
53 vegetation changes may also contribute to recent trends in West African dust (Chiapello, 2005;  
54 Evan et al., 2011). Since the 1950s, dust emissions from Africa have increased (Evan and  
55 Mukhopadhyay, 2010; Mbourou et al., 1997; Prospero et al., 2002), peaking in the 1980s at the  
56 same time as the extreme droughts experienced in the Sahel region. During this period a robust  
57 correlation was observed between dust transported to Barbados in the summer and Soudano –  
58 Sahel Precipitation Index of the previous year (Prospero and Lamb, 2003). In the past three  
59 decades, observations from satellite and surface measurements indicate a breakdown in this  
60 relationship (Mahowald et al., 2009), and a decrease in dustiness (Chin et al., 2013; Evan and  
61 Mukhopadhyay, 2010; Hsu et al., 2012; Shao et al., 2013; Zhao et al., 2008) coinciding with a  
62 greening of the Sahel region (Olsson et al., 2005). A vegetation-related increase in surface  
63 roughness may also have contributed to the stilling of winds (and corresponding reduction in  
64 dust) over much of the Northern Hemisphere (Vautard et al., 2010; Bichet et al., 2012), including  
65 the Sahel region (Cowie et al., 2013).

66 Modeling studies generally agree that changes in precipitation over the Sahel, leading to the  
67 drought and subsequent greening, can be explained by changes in the inter-hemispheric

68 temperature gradient across the Atlantic (Chiang and Friedman, 2012; Hwang et al., 2013;  
69 Rotstayn and Lohmann, 2002; Zhang and Delworth, 2006) which influences the location of the  
70 Inter-Tropical Convergence Zone (ITCZ). Changes in dust emissions and transport over the  
71 Atlantic are associated with the location of the ITCZ (Doherty et al., 2012; Fontaine et al., 2011)  
72 which may provide a feedback by modulating the radiative balance over the Atlantic (Evan et al.,  
73 2011). However, whether the observed changes in dust are a direct consequence of the large-  
74 scale changes associated with the ITCZ location or a consequence of the greening of the Sahel,  
75 either via a reduction in available dust sources or a stilling of the surface winds, is still unclear.

76 Dust outflow from Africa is somewhat correlated with the North Atlantic Oscillation (NAO) based  
77 on comparison with observations (Chiapello, 2005; Moulin et al., 1997, p.199; Nakamae and  
78 Shiotani, 2013) with the strongest relationship north of 15°N (Chiapello and Moulin, 2002). The  
79 NAO index, defined by the difference in normalized sea level pressure between the Icelandic low  
80 and Azores high (Hurrell, 1995), is extremely noisy and our understanding of what causes the  
81 fluctuations is limited (Stephenson et al., 2000). While the NAO index represents changes in  
82 circulation that affect dust transport, primarily via the Azores high rather than Icelandic low  
83 (Riemer et al., 2006), the correlation with observations of dust close to source regions is weak  
84 (Nakamae and Shiotani, 2013). Therefore, we choose to focus primarily on the physical processes  
85 the drive dust emission and export (e.g. wind strength and precipitation) rather than the climate  
86 indices that may represent them.

87 In this paper we use surface and satellite dust observations along with a 27 year model simulation  
88 to quantify the driving factors behind the variability and trends in dust loading over the Atlantic,  
89 the importance of vegetation changes for dust emission, and whether the underlying causes are

90 natural or anthropogenic in origin. The magnitude of modeled and observed variability and  
91 trends in Atlantic dust AOD and direct radiative effect (DRE) are assessed and the causes  
92 quantified using the model. Finally, we discuss a potential driver of changes in surface winds using  
93 three reanalysis datasets and fifteen CMIP5 model simulations.

94

## 95 **2. Model description and evaluation**

### 96 **2.1 Baseline model description**

97 The GEOS-Chem model (version v9-01-01; <http://www.geos-chem.org/>) incorporates a global  
98 three-dimensional simulation of coupled oxidant-aerosol chemistry, run at a resolution of 2° x  
99 2.5° latitude and longitude, and 47 vertical levels in this study. The model is driven by assimilated  
100 MERRA meteorology for 1982-2008 from the Goddard Earth Observing System of the NASA  
101 Global Modeling and Assimilation Office (GMAO), which includes assimilated meteorological  
102 fields at 1-hourly and 3-hourly temporal resolution. The aerosol types simulated include mineral  
103 dust (Fairlie et al., 2007; Zender et al., 2003), sea salt (Alexander et al., 2005), sulfate-nitrate-  
104 ammonium aerosols (Park et al., 2004), and carbonaceous aerosols (Henze et al., 2008; Liao et  
105 al., 2007; Park et al., 2003). Aerosol optical depth (AOD) is calculated online assuming lognormal  
106 size distributions of externally mixed aerosols and is a function of the local relative humidity to  
107 account for hygroscopic growth (Martin et al., 2003). Aerosol optical properties employed here  
108 are based on the Global Aerosol Data Set (GADS) (Kopke et al., 1997) with modifications to the  
109 size distribution based on field observations (Drury et al., 2010; Jaegle et al., 2010; Ridley et al.,  
110 2012) and to the refractive index of dust (Sinyuk et al., 2003).

111 For all long-term simulations in this study the standard model is modified to include dust aerosol  
112 only. Emission, dry deposition and wet scavenging of dust are all simulated as in the standard  
113 model (Fairlie et al., 2007). Dust emission in GEOS-Chem is based upon the DEAD dust scheme  
114 (Zender et al., 2003), making use of the GOCART source function (Ginoux et al., 2001) as proposed  
115 by Fairlie et al. (2007), based on evaluation of dust concentrations over the US. Mineral dust mass  
116 is transported in four size bins (0.1 - 1.0, 1.0 - 1.8, 1.8 - 3.0 and 3.0 - 6.0  $\mu\text{m}$ ), the smallest of which  
117 is partitioned into four bins (0.10 - 0.18, 0.18 - 0.30, 0.30 - 0.65 and 0.65 - 1.00  $\mu\text{m}$ ) when deriving  
118 optical properties, owing to the strong size-dependence of extinction for sub-micron aerosol  
119 (Ridley et al., 2012).

120 The GEOS-Chem model has been coupled with RRTMG, a rapid radiative transfer model (Mlawer  
121 et al., 1997), to quantify the DRE of aerosol species online (Heald et al., 2013). In this version of  
122 the model we calculate the shortwave (SW) and longwave (LW) radiative effects for dust based  
123 on fluxes at 30 wavelengths under both clear-sky and all-sky conditions.

124

## 125 **2.2 Dust emission scheme updates**

126 Two significant changes have been made to the dust scheme relative to the standard GEOS-Chem  
127 implementation described thus far. First, we account for sub-grid variability in surface winds and,  
128 second, we alter the dust source function to depend on geomorphology and include dynamic  
129 vegetation cover. We represent the sub-grid winds as a Weibull probability density function  
130 based on statistics derived from the native resolution of the assimilated meteorology wind fields  
131 ( $0.5^\circ \times 0.67^\circ$ ). We previously showed that accounting for the sub-grid wind distribution reduces

132 the resolution-dependence of dust emissions in the model by better representing situations  
133 when the mean wind speed is approaching the threshold for dust activation (Ridley et al., 2013).  
134 To investigate the role of vegetation changes in modulating dust emissions we must simulate  
135 dust emission from semi-arid regions. Compared to more recent dust source region studies  
136 (Ginoux et al., 2012; Koven and Fung, 2008; Schepanski et al., 2007) the original GOCART dust  
137 source derived from TOMS aerosol index is likely to underestimate emissions from regions that  
138 are not permanent deserts. Satellite-derived dust source data sets often disagree as a result of  
139 cloud cover and temporal sampling, particularly in regions where emissions show distinct diurnal  
140 patterns, such as West Africa (Schepanski et al., 2012). For this reason we implement the  
141 geomorphic dust source map of Koven et al. (2008), derived from surface roughness and  
142 levelness properties, and let vegetation cover attenuate the source strength. We follow (Kim et  
143 al., 2013) in deriving the bareness fraction from AVHRR Normalized Difference Vegetation Index  
144 (NDVI) for each year (values  $<0.15$  are considered bare and a potential dust source) to modulate  
145 dust emissions from 1982-2008. The updated dust scheme performs at least as well as the  
146 original dust scheme when assessed relative to MODIS and AERONET observations over Africa  
147 and the mid-Atlantic (see supplementary material). The relatively small change in agreement  
148 even with substantial changes in source regions suggests that the wind fields dominate the  
149 agreement with observations, both in terms of the surface wind strength leading to emissions  
150 and the large-scale transport across the continent. Achieving a higher fidelity dust simulation  
151 therefore appears to rely more on an improvement of the wind fields than the characterization  
152 of the surface properties.

153

### 154 **2.3 Regional direct radiative effect (DRE)**

155 Using the updated GEOS-Chem model coupled with RRTMG we quantify the change in radiative  
156 flux at the surface resulting from the changes in dust aerosol over the 27 year period (for all-sky  
157 conditions). Figure 1 shows the average seasonal DRE of dust over Africa and the Atlantic for the  
158 whole 27 year period, both at surface and TOA. We define the radiative effect as an increase in  
159 down-welling flux and therefore a negative value constitutes a cooling of the Earth. Globally, the  
160 all-sky radiative effect from African dust is  $-0.18 \text{ Wm}^{-2}$  at TOA, accounting for 46% of the total  
161 global dust DRE. Across the mid-Atlantic ( $5 - 20^{\circ}\text{N}$ ,  $10 - 50^{\circ}\text{W}$ ) the mean annual radiative effect  
162 of dust is  $-3.2 \pm 0.7 \text{ Wm}^{-2}$  at TOA and  $-7.4 \pm 1.5 \text{ Wm}^{-2}$  at the surface, including LW contributions  
163 of  $+0.4 \pm 0.1 \text{ Wm}^{-2}$  and  $+3.1 \pm 0.7 \text{ Wm}^{-2}$ , respectively. This region covers less than 5% of the Earth's  
164 surface but accounts for almost 20% of the global dust radiative effect at TOA and at the surface.  
165 The difference between the TOA and surface radiative effects indicates the heating of the  
166 atmosphere owing to dust. When the dust outflow is over the Sahara (primarily during summer)  
167 the airborne dust can be darker than the surface beneath, decreasing the amount of outgoing  
168 radiation and producing a warming effect at TOA.

169 While direct comparison with previous estimates is difficult owing to different time periods,  
170 conditions and model assumptions, we find the spatial distribution and magnitude of the DRE is  
171 broadly consistent with previous modeling studies (Evan and Mukhopadhyay, 2010; Miller et al.,  
172 2004; Yoshioka et al., 2007) and observations (Haywood et al., 2003; Highwood, 2003; Hsu et al.,  
173 2000). Aerosol size, shape refractive index, altitude, and surface albedo all contribute to the  
174 uncertainty in the radiative effect and lead to considerable diversity between models and  
175 observations. Several studies have attempted to quantify the key factors leading to uncertainty



176 in radiative effect and radiative forcing (e.g. (Balkanski et al., 2007; Evan et al., 2009; Miller et al.,  
177 2004; Myhre et al., 2013; Stier et al., 2013) but this is certainly an area requiring further research  
178 to better constrain model estimates.

179

### 180 **3. Observations**

181 The primary long-term observations used in this study is a dust AOD (DAOD) dataset over the  
182 mid-Atlantic for the period 1982 – 2008, derived from satellite observations by (Evan and  
183 Mukhopadhyay, 2010). Satellite retrievals of AOD from the AVHRR PATMOS-x dataset, an  
184 extended and recalibrated retrieval using the moderate resolution imaging spectro-radiometer  
185 (MODIS) observations (Zhao et al., 2008), are converted to DAOD using MODIS AOD and fine  
186 mode fraction products and with NCEP-NCAR reanalysis surface winds, following Kaufman et al.  
187 (2005). The 1° x 1° DAOD product is only available over the ocean, between 0 - 30°N and 65 -  
188 10°W, therefore we select three 7.5° by 10° regions representing outflow towards North America,  
189 the Caribbean, and South America in which to compare model and observations (see Fig. 2). We  
190 also consider a 10° by 17.5° region off the coast of Africa to assess outflow close to source; initially  
191 this region was divided into two, north and south of Cape Verde; however, the results are largely  
192 the same when considering the region as a whole.

193 Trade-wind aerosol has been measured almost continually at the Ragged Point site on the east  
194 coast of Barbados since 1965 (Prospero and Lamb, 2003). During conditions when the on shore  
195 wind exceeds 1 ms<sup>-1</sup> (~95% of the time, (Savoie et al., 1989) air is drawn through a filter upon a  
196 20m tower, the soluble material is removed and the remaining mineral residue (representing the

197 dust aerosol) weighed after ashing. We use monthly average dust concentrations for the period  
198 1982 – 2008 to evaluate long range dust transport from Africa.

199 Rather than the standard Boreal seasonal classification (DJF and JJA) we follow the work of (Ben-  
200 Ami et al., 2012) who show that African dust seasonality can be broken down into three seasons:  
201 December to March, April to mid-October, and October through November. Throughout this  
202 study we compare the modeled and observed DAOD and surface concentrations either annually  
203 or for two seasons, referred to as winter (DJFM) and summer (AMJJAS). The October-November  
204 period is characterized by low dust emission and is not shown separately, but included in the  
205 annual averages.

206

## 207 **4. Dust Transport and Trends**

208

### 209 **4.1 Trends and variability in dustiness and the radiative effect**

210 To assess how the dust loading over the mid-Atlantic has changed since the 1980s and whether  
211 the model captures the observed variability we consider the DAOD derived from satellite data in  
212 regions close to source and further downwind. Figure 3 shows the seasonally-averaged DAOD for  
213 the model and derived from satellite observations in each of the outflow regions indicated in Fig.  
214 2 from 1982 to 2008. The DAOD is displayed as an anomaly from the climatological average for  
215 the winter and summer seasons.

216 Close to source, the model captures 50 - 80% of the variance in the observations in the winter  
217 months (monthly correlations between 0.69 and 0.90). The seasonal correlation with the  
218 observations is fair during summer ( $r = 0.64$ ) with the model struggling to represent the variability

219 and magnitude of emissions between June and August; likely a consequence of underestimated  
220 AOD at the Bodélé Depression and across the Sahel during summer (see Supplementary Fig. S2).  
221 Downwind, correlations between model and observations range between 0.46 and 0.65  
222 (excluding the North America region during winter when very little dust is present). The poorer  
223 agreement downwind indicates that model transport and removal contribute to the discrepancy  
224 with observations. The variability in the model DAOD is generally less than observed, owing to  
225 lower model DAOD; however, the normalized variability (normalizing using the climatological  
226 mean DAOD) is comparable between model and observations. Previous studies have shown that  
227 the model removes dust aerosol too rapidly relative to the observations via both wet and dry  
228 deposition (Generoso et al., 2008; Ridley et al., 2012) and this is likely to be contributing to the  
229 reduced variability in DAOD at these downwind regions. Overall we see best agreement for  
230 seasons with the highest dust loading, i.e. winter at the South America region and summer in the  
231 Caribbean and North Atlantic regions.

232 Significant decreasing trends in observed DAOD (>95% confidence) are apparent for all seasons  
233 and locations, except winter in the North America and Caribbean regions when northerly  
234 transport of dust is limited and highly variable, respectively. There are striking similarities  
235 between the trends in observed and modeled DAOD, with the model showing significant trends  
236 at the same locations and during the same seasons. Annually, observed and modeled DAOD  
237 decreases between -0.035 (12%) and -0.032 (17%) per decade close to source and -0.021 (12%)  
238 to -0.016 (28%) per decade downwind, respectively. Previous studies show similar decreases of  
239 total AOD per decade in the mid-Atlantic based on the AVHRR PATMOS-x dataset (Mishchenko  
240 and Geogdzhayev, 2007; Zhao et al., 2008) and SeaWIFs observations from 1997 – 2010 (Hsu et

241 al., 2012). This suggests that the trends in total AOD over the mid-Atlantic are driven almost  
242 entirely by the changes in dust aerosol.

243 There is significant interannual variability in dust concentration during the spring months (March  
244 – May), a period responsible for transport of dust to South America based on both satellite and  
245 in-situ measurements (Kaufman et al., 2005a; Prospero et al., Submitted, 1981). Isolating the  
246 spring season we find significant trends in DAOD of -0.02 per decade for both observations and  
247 model in the South America region ( $r=0.70$ ) indicating that the decreasing dust trends are present  
248 and captured by the model in this season as well as the broader seasons considered in this study.  
249 Figure 4 shows the anomaly in monthly dust concentration measured at Barbados alongside the  
250 modeled surface concentration anomaly. We find that seasonal correlation between the dust  
251 surface concentration measured at Barbados and simulated concentrations show similar  
252 agreement as the DAOD comparisons, with  $r = 0.69$  and  $r = 0.44$  during winter and summer,  
253 respectively. Surface concentration of dust measured at Barbados has been decreasing during  
254 the summer ( $-3.5 \pm 1.3 \mu\text{gm}^{-3}$  per decade); this trend is reproduced by the model ( $-5.2 \pm 1.1 \mu\text{gm}^{-3}$   
255 per decade). No trend is present in either observations or model during the winter, consistent  
256 with the Caribbean regional DAOD (Fig. 3).

257 The consistency and geographical extent of the downward trends in both the modeled and  
258 observed dust suggest that the model simulates the process driving these trends in dust  
259 throughout this multi-decadal period.

260 The inset charts within Fig. 1 show the modeled time series of seasonal DRE for the region  $0^\circ\text{N} -$   
261  $30^\circ\text{N}$ ,  $50^\circ\text{W} - 15^\circ\text{E}$ , encompassing the mid-Atlantic and West Africa. We note considerable  
262 variability in the radiative effect from year to year, primarily in winter when emissions are more

263 sporadic in the model, confirmed by observations (Ben-Ami et al., 2012). The regional surface  
264 cooling varies by up to  $8 \text{ Wm}^{-2}$  in winter and  $6 \text{ Wm}^{-2}$  in summer, and a more modest  $4 \text{ Wm}^{-2}$  and  
265  $1.5 \text{ Wm}^{-2}$  at TOA in winter and summer, respectively. Annually, warming trends of  $+1.27 \text{ Wm}^{-2}$   
266 and  $+0.37 \text{ Wm}^{-2}$  per decade are observed at the surface and TOA, respectively, over the region  
267 including both the ocean and land from 1982 to 2008. The seasonal trends are similar in  
268 magnitude, with significant trends in both winter and summer (95% confidence). Similar trends  
269 in DRE exist over both ocean and land at the surface ( $+1.23 \text{ Wm}^{-2}$  and  $+1.32 \text{ Wm}^{-2}$  per decade,  
270 respectively) but at TOA there are marked differences between the trends over ocean and land  
271 ( $+0.60 \text{ Wm}^{-2}$  and  $+0.00 \text{ Wm}^{-2}$  per decade) as a result of surface albedo and the high concentration  
272 of large dust particles (increasing the LW warming effect). The regional trend constitutes an  
273 increase in DRE over the past three decades that is comparable in magnitude to the regional  
274 increase in  $\text{CO}_2$  forcing since 1750 (Stocker et al., n.d.). This illustrates the strong radiative  
275 perturbation potential of dust: climatic changes that are affecting the emission of African dust  
276 are likely to have significant impacts upon the radiative balance over the Atlantic that are not  
277 accounted for in the traditional radiative forcing metric.

278

#### 279 **4.2 Attribution of variability and trends in dustiness**

280 To attribute the driving forces behind the interannual variability in African dust near source and  
281 downwind, four 27 year simulations are performed with interannual variability removed from  
282 surface winds, transport, precipitation, or vegetation. This method also removes any inter-annual  
283 trend in that variable. The interannual variability of 10-m surface winds are removed by using the  
284 1988 10-m winds for every year, 1988 being an 'average' year in terms of dust emissions (N.B.

285 this only affects the 10-m winds used for calculation of dust emission flux, not for other processes  
286 in the model). This process is repeated by holding vegetation constant at 1988 values or by fixing  
287 precipitation and 3-D winds (other than 10-m surface winds) to 1988 values for the 27 year  
288 period. Here we are investigating only the direct impact of vegetation cover reducing available  
289 surface for dust emission and do not take into account secondary effects such as stilling of winds  
290 from surface roughness changes, discussed further below.

291 The variability caused by each of the three factors is inferred by assessing the reduction in the  
292 variance of the DAOD in each region relative to the original model. This method does not account  
293 for confounding factors resulting from the variables being dependent (i.e. the large scale winds  
294 and 10-m wind strength will be well correlated) but results are found to be robust (within  $\pm 5\%$ )  
295 when removing the interannual variability using data from 2004 instead of 1988. Figure 5 shows  
296 the apportionment of variability in DAOD to the three factors tested for summer and winter. In  
297 the coastal Africa and South America regions the 10-m surface wind accounts for at least two  
298 thirds of the variability in both seasons. In North America and the Caribbean surface winds  
299 account for one third to half of the variability in the DAOD, interannual variability in large-scale  
300 transport being more important during the winter. Precipitation accounts for only a small fraction  
301 of the variability in DAOD in all regions during the winter, but becomes more important  
302 downwind during the summer. Within the model, precipitation primarily affects the variability in  
303 dust loading over the Atlantic via wet scavenging rather than by increasing soil wetness and  
304 suppressing emission. Removing the interannual variability of vegetation has a negligible impact  
305 on the variability in DAOD suggesting that the changes in dust source region resulting from  
306 vegetation cover changes are unimportant for the observed variability in dust since the 1980s.

307 The same four simulations described above are used to assess the cause of trends in DAOD.  
308 Figure 6 shows the resulting annual DAOD anomaly in each region for each simulation. In the  
309 Coastal Africa region it is clear that removing interannual variability in 10-m winds almost entirely  
310 removes the trend in DAOD. Further downwind the interannual variability in other meteorology  
311 contributes between 30 – 50% of the trend; however, the surface wind at source remains the  
312 dominant driver. This indicates that, in the model, the trend in dustiness results from a stilling of  
313 surface winds over source regions and combines with changes in transport and/or an increase in  
314 removal downwind, more so in the more northerly outflow regions. We find that the direct effect  
315 of vegetation changes on dust emission in the model has a negligible impact on the trend in  
316 dustiness over the Atlantic. In all locations except North America the trend with no interannual  
317 variability in 10-m surface winds is significantly different to the baseline run (>95% confidence),  
318 whereas the trend with no interannual variability in vegetation is indistinguishable from the  
319 baseline. Although surface winds have been inferred as the likely cause of the observed reduction  
320 in Atlantic dust loading (Chin et al., 2013) this is the first time that the link has been quantified.  
321 While we do find a positive correlation between the NAO index and the DAOD in the outflow  
322 regions during winter, we find no significant trend in the NAO index between 1982 and 2008,  
323 therefore the question remains as to what is driving the stilling of winds over Africa. We have  
324 shown that changes in vegetation are unlikely to *directly* influence dust emission via changes in  
325 source regions but they may still indirectly affect the emissions via stilling of the winds. If  
326 vegetation changes are driving the decrease in winds responsible for the change in dustiness over  
327 the Atlantic then any increase in vegetation cover is expected to be coincident with the decrease  
328 in winds (Bichet et al., 2012).

329 Figure 7a shows the change in the bareness fraction (a reduction in bareness fraction indicating  
330 a 'greening') derived from AVHRR between 1982-1986 and 2002-2006 for summer and winter.  
331 Figure 7b shows the change in surface winds apparent in the MERRA reanalysis and the regions  
332 in which dust emissions decrease by more than 0.5 Tg per grid box. For both seasons we see that  
333 there is a limited amount of overlap between the location in which vegetation increases and the  
334 surface winds (and therefore emissions) decrease. This is not necessarily in disagreement with  
335 the conclusions of Cowie et al. (2013); there the focus is on local Sahelian emissions only. Events  
336 when dust is transported from elsewhere are excluded and account for between 50% and 90%  
337 of all dust events at the Sahel weather stations (personal comm. Sophie Cowie). The reanalysis  
338 winds are unlikely to capture the full extent of wind stilling from surface roughness changes and  
339 therefore may be missing trends in winds and dust emission in the Sahel. However, the model  
340 still captures the decreasing trends in dust over the Atlantic, suggesting that emissions from  
341 regions other than the Sahel are controlling the trends in Atlantic DAOD. The lack of spatial  
342 correspondence between the greening and the wind stilling indicate that vegetation is not driving  
343 the change in model surface winds though perhaps both are the result of a larger-scale climatic  
344 change. Indeed, shifts in dustiness over the past 20,000 years also suggest that large changes in  
345 dust emission in the past are primarily driven by changes in large-scale winds, rather than  
346 vegetation and precipitation changes (McGee et al., 2010).

347

#### 348 **4.3 Reliability of surface wind trends in reanalyses**

349 To assess the reliability of the MERRA surface winds in this relatively observation-poor region we  
350 compare annual MERRA reanalysis wind trends between 1982 and 2008 with those from the



351 NCEP and ERA-Interim reanalysis products. Figure 8 shows the annual trend in winds for the three  
352 reanalyses over the region of interest with trends that are significant at the 95% confidence level  
353 indicated. The broad trends across the Atlantic are consistent between the reanalyses, primarily  
354 a significant stilling between 10 – 20°N and a strengthening of the wind in the Gulf of Guinea and  
355 south of the equator. Across North Africa, all three reanalyses show significant stilling in regions  
356 associated with dust production. The trends in MERRA are generally stronger than observed in  
357 the two other reanalysis products; however, it has been shown that NCEP and ERA-Interim  
358 reanalysis wind trends are weaker than trends in surface observations (Cowie et al., 2013;  
359 Vautard et al., 2010) and therefore the stronger trend in MERRA is expected to agree better with  
360 the surface observations. There is some disagreement in the latitude and strength of the stilling  
361 over the dust source regions but the consistency in the significant stilling trends between  
362 reanalysis products bolsters confidence in the MERRA surface wind trends.

363

364

## 365 **5. Potential mechanism to explain the trends in African dust**

366 Thus far, we have shown that the trends in North African dust are driven by stilling of the surface  
367 wind, more likely from large-scale changes in circulation than the result of land-use and  
368 vegetation changes. Here we consider a potential mechanism that may explain the recent trend.  
369 Booth et al. (2012) have shown that changes in aerosol indirect effects over the North Atlantic,  
370 primarily driven by anthropogenic aerosol, may play a key role in modulating the North Atlantic  
371 sea surface temperature (SST) and that aerosol changes may be the source of the Atlantic  
372 Multidecadal Oscillation (AMO) that is often shown to correlate with African dust concentrations

373 (Chin et al., 2013; Shao et al., 2013; Wang et al., 2012). Several studies have shown a southward  
374 displacement of the inter-tropical convergence zone (ITCZ) in response to a decrease in the North  
375 Atlantic SST (Broccoli et al., 2006; Rotstayn and Lohmann, 2002; Williams et al., 2001). While  
376 these studies generally consider the implications in terms of the change in precipitation and  
377 drought in the Sahel, the location of the ITCZ is associated with changes in the wind strength and  
378 direction over North Africa as well (Doherty et al., 2012; Fontaine et al., 2011). A warming of the  
379 North Atlantic is expected to produce a northward shift (or broadening) in the ITCZ, bringing more  
380 precipitation to the Sahel and also associated with decreasing wind strength, and therefore both  
381 a vegetative greening and a reduction in dust emissions, as observed. This presents a potentially  
382 important connection between anthropogenic aerosol loading in the Northern mid-latitudes and  
383 changes in African dust emissions.

384 While it is beyond the scope of this paper to investigate the cause of large-scale wind changes  
385 (GEOS-Chem is not a coupled climate model), we present a brief analysis of surface winds from  
386 the CMIP5 models and reanalysis products. Using monthly mean surface wind output from fifteen  
387 CMIP5 'historical' simulations we derive surface wind trends for 1982 – 2008 over Africa and the  
388 Mid-Atlantic and compare these with the average trend from the three meteorological  
389 reanalysis. The surface wind trends in the CMIP5 models over Africa and the Atlantic do not  
390 match the reanalysis products, with spatial correlations varying between -0.3 and 0.3. However,  
391 each of the models considered contain atmospheric modules of differing complexity and may  
392 capture different processes. To investigate the potential link between the aerosol indirect effect  
393 (AIE) and surface wind trends we group the models based upon whether or not they include  
394 aerosol feedback upon cloud properties, i.e. the aerosol indirect effect, required to model

395 observed SST changes in (Booth et al., 2012). Eight are found to include a parameterization for  
396 the feedback and seven do not. Using bootstrapping, we randomly sample three models 500  
397 times, obtain the trend in surface winds from the ensemble, and calculate the spatial correlation  
398 with the reanalysis products over the North Africa / Atlantic region. Figure 9 shows the  
399 distribution of correlation coefficients for all samples and for subsets with only those models  
400 containing the AIE and those without AIE. We find that when the sample contains only those  
401 models known to represent the aerosol indirect effect the correlation with reanalysis surface  
402 wind trends is better than 91% of the other random samples, with a mean correlation of 0.16 (-  
403 0.05 to 0.29). Furthermore, when the sample contains only those models known to not contain  
404 the aerosol indirect effect the correlation is worse than 90% of the random samples, correlation  
405 of -0.08 (-0.22 to 0.13). While these correlations are extremely weak, the results with and without  
406 aerosol indirect effect are significantly different to one another (greater than 99% confidence)  
407 and to the mean of all the randomized samples (0.05), indicating there may be a link between  
408 simulating the indirect effect of aerosols and better representation of trends in surface winds, as  
409 represented by the assimilated meteorology.

410

## 411 **6. Summary and Conclusions**

412 This research and previous studies have found that satellite observations across the Atlantic  
413 show a significant downward trend in DAOD since the 1980s, persisting through both summer  
414 and winter seasons. We also observe decreasing trends in surface dust concentrations at  
415 Barbados during summer. The GEOS-Chem model captures the broad trends in dustiness over  
416 the Atlantic and we estimate that they lead to an annually averaged warming of  $+1.23 \text{ Wm}^{-2}$  per

417 decade over the surface of the mid-Atlantic since 1982. We find that the trends are driven  
418 primarily by a reduction in surface winds in regions that are unlikely to be associated with  
419 vegetation cover changes. This suggests that the change in African dust emissions since the 1980s  
420 cannot be directly attributed to vegetation changes (including anthropogenic land use changes  
421 in the Sahel region); therefore, a vegetation feedback on dust emission via surface roughness  
422 may be valid on a local scale but appears less important for dust sources responsible for the  
423 trends in dustiness over the Atlantic.

424 Along with isolating the cause of the trends, the drivers of interannual variability in dustiness  
425 over the Atlantic have been investigated. We find that the interannual variability is primarily  
426 controlled by changes in surface winds over Africa, accounting for 60 - 80% of the interannual  
427 variability in dust AOD off the coast of Africa. Further downwind, transport and (to a lesser  
428 extent) precipitation contribute 30 - 60% and 0 - 15% to the variability in dust AOD, respectively,  
429 depending upon season. Using the model we find that the variability in dust leads to substantial  
430 interannual changes in surface insolation of over  $6.0 \text{ Wm}^{-2}$ , averaged over the mid-Atlantic. These  
431 are likely to have a significant impact on heating of the ocean mixed layer therefore and tropical  
432 storm genesis (Evan et al., 2009), highlighting the importance of well-characterized variability in  
433 dust emissions in climate models.

434 Finally, we propose a potential connection between anthropogenic aerosol loading over the  
435 North Atlantic and the trends in dustiness in the mid-Atlantic. The link between the aerosol direct  
436 and indirect effects over the North Atlantic and changes in the SST and ITCZ are well established.  
437 We take this one step further and suggest that the wind stilling over Africa, reducing dustiness  
438 over the Atlantic in recent decades, may be a further consequence of these interactions. The

439 CMIP5 models do not capture the wind trend over Africa, preventing conclusive evidence of this  
440 mechanism. However, the CMIP5 models that include aerosol indirect effects show significantly  
441 better agreement with surface wind trends in reanalysis meteorology than those without indirect  
442 aerosol effects, offering evidence that the aerosol indirect effect may be critical to the prediction  
443 of surface winds trends over Africa. This is a potentially important anthropogenic aerosol driver  
444 upon 'natural' dust aerosol via climate, capable of amplifying the climate sensitivity to  
445 anthropogenic aerosol in the Atlantic, which is not captured by the aerosol radiative forcing  
446 metric.

447

#### 448 **Acknowledgements**

449 The authors would like to thank Charlie Koven for the dust source function, Amato Evan for the  
450 satellite-derived dust AOD product, John Marsham and Sophie Cowie for providing data on the  
451 dust source classification, Kerstin Schepanski for supplying dust activation data derived from  
452 SEVIRI, and Owen Doherty for discussions and data relating to the ITCZ. This work was funded  
453 by the MIT Charles E. Reed Faculty Initiative Fund and the National Science Foundation (AGS-  
454 1238109). The Barbados research is funded with grants to J. M. Prospero from the National  
455 Science Foundation AGS-0962256 and NASA NNX12AP45G.

456

#### 457 **Bibliography**

458 Alexander, B., Park, R. J., Jacob, D. J., Li, Q. B., Yantosca, R. M., Savarino, J., Lee, C. C. W. and Thiemens,  
459 M. H.: Sulfate formation in sea-salt aerosols: Constraints from oxygen isotopes, *J. Geophys. Res.-*  
460 *Atmospheres*, 110(D10), doi:10.1029/2004JD005659, doi:D10307 Artn d10307, 2005.

461 Ben-Ami, Y., Koren, I., Altaratz, O., Kostinski, A. and Lehahn, Y.: Discernible rhythm in the  
462 spatio/temporal distributions of transatlantic dust, *Atmospheric Chem. Phys.*, 12(5), 2253–2262,  
463 doi:10.5194/acp-12-2253-2012, 2012.

464 Balkanski, Y., Schulz, M., Claquin, T. and Guibert, S.: Reevaluation of Mineral aerosol radiative forcings  
465 suggests a better agreement with satellite and AERONET data, *Atmospheric Chem. Phys.*, 7, 81–95,  
466 2007.

467 Bichet, A., Wild, M., Folini, D. and Schär, C.: Causes for decadal variations of wind speed over land:  
468 Sensitivity studies with a global climate model: Decadal variations of land wind speed, *Geophys. Res.*  
469 *Let.*, 39(11), doi:10.1029/2012GL051685, 2012.

470 Booth, B. B. B., Dunstone, N. J., Halloran, P. R., Andrews, T. and Bellouin, N.: Aerosols implicated as a  
471 prime driver of twentieth-century North Atlantic climate variability, *Nature*, 484(7393), 228–232,  
472 doi:10.1038/nature10946, 2012.

473 Broccoli, A. J., Dahl, K. A. and Stouffer, R. J.: Response of the ITCZ to Northern Hemisphere cooling,  
474 *Geophys. Res. Let.*, 33(1), doi:10.1029/2005GL024546, 2006.

475 Chiang, J. C. H. and Friedman, A. R.: Extratropical Cooling, Interhemispheric Thermal Gradients, and  
476 Tropical Climate Change, *Annu. Rev. Earth Planet. Sci.*, 40(1), 383–412, doi:10.1146/annurev-earth-  
477 042711-105545, 2012.

478 Chiapello, I.: Understanding the long-term variability of African dust transport across the Atlantic as  
479 recorded in both Barbados surface concentrations and large-scale Total Ozone Mapping Spectrometer  
480 (TOMS) optical thickness, *J. Geophys. Res.*, 110(D18), doi:10.1029/2004JD005132, 2005.

481 Chiapello, I. and Moulin, C.: TOMS and METEOSAT satellite records of the variability of Saharan dust  
482 transport over the Atlantic during the last two decades (1979–1997), *Geophys. Res. Let.*, 29(8), 17–1–  
483 17–4, doi:10.1029/2001GL013767, 2002.

484 Chin, M., Diehl, T., Tan, Q., Prospero, J. M., Kahn, R. A., Remer, L. A., Yu, H., Sayer, A. M., Bian, H.,  
485 Geogdzhayev, I. V., Holben, B. N., Howell, S. G., Huebert, B. J., Hsu, N. C., Kim, D., Kucsera, T. L., Levy, R.  
486 C., Mishchenko, M. I., Pan, X., Quinn, P. K., Schuster, G. L., Streets, D. G., Strode, S. A., Torres, O. and  
487 Zhao, X.-P.: Multi-decadal variations of atmospheric aerosols from 1980 to 2009: sources and regional  
488 trends, *Atmospheric Chem. Phys. Discuss.*, 13(7), 19751–19835, doi:10.5194/acpd-13-19751-2013, 2013.

489 Cowie, S. M., Knippertz, P. and Marsham, J. H.: Are vegetation-related roughness changes the cause of  
490 the recent decrease in dust emission from the Sahel?, *Geophys. Res. Let.*, 40(9), 1868–1872,  
491 doi:10.1002/grl.50273, 2013.

492 Doherty, O. M., Riemer, N. and Hameed, S.: Control of Saharan mineral dust transport to Barbados in  
493 winter by the Intertropical Convergence Zone over West Africa: Winter dust in Barbados and the ITCZ, *J.*  
494 *Geophys. Res. Atmospheres*, 117(D19), doi:10.1029/2012JD017767, 2012.

495 Drury, E., Jacob, D. J., Spurr, R. J. ., Wang, J., Shinozuka, Y., Anderson, B. E., Clarke, A. D., Dibb, J.,  
496 McNaughton, C. and Weber, R.: Synthesis of satellite (MODIS), aircraft (ICARTT), and surface (IMPROVE,  
497 EPA-AQS, AERONET) aerosol observations over eastern North America to improve MODIS aerosol  
498 retrievals and constrain surface aerosol concentrations and sources, *J. Geophys. Res.*, 115(D14), D14204,  
499 2010.

500 Dunion, J. P. and Velden, C. S.: The Impact of the Saharan Air Layer on Atlantic Tropical Cyclone Activity,  
501 *Bull. Am. Meteorol. Soc.*, 85(3), 353–365, doi:10.1175/BAMS-85-3-353, 2004.

502 Evan, A. T., Dunion, J., Foley, J. A., Heidinger, A. K. and Velden, C. S.: New evidence for a relationship  
503 between Atlantic tropical cyclone activity and African dust outbreaks, *Geophys. Res. Lett.*, 33(19),  
504 doi:10.1029/2006GL026408, 2006.

505 Evan, A. T., Foltz, G. R., Zhang, D. and Vimont, D. J.: Influence of African dust on ocean–atmosphere  
506 variability in the tropical Atlantic, *Nat. Geosci.*, 4(11), 762–765, doi:10.1038/ngeo1276, 2011.

507 Evan, A. T. and Mukhopadhyay, S.: African Dust over the Northern Tropical Atlantic: 1955–2008, *J. Appl.*  
508 *Meteorol. Climatol.*, 49(11), 2213–2229, doi:10.1175/2010JAMC2485.1, 2010.

509 Evan, A. T., Vimont, D. J., Heidinger, A. K., Kossin, J. P. and Bennartz, R.: The Role of Aerosols in the  
510 Evolution of Tropical North Atlantic Ocean Temperature Anomalies, *Science*, 324(5928), 778–781,  
511 doi:10.1126/science.1167404, 2009.

512 Fairlie, T. D., Jacob, D. J. and Park, R. J.: The impact of transpacific transport of mineral dust in the United  
513 States, *Atmos. Environ.*, 41(6), 1251–1266, doi:10.1016/j.atmosenv.2006.09.048, 2007.

514 Fontaine, B., Roucou, P., Gaetani, M. and Marteau, R.: Recent changes in precipitation, ITCZ convection  
515 and northern tropical circulation over North Africa (1979–2007), *Int. J. Climatol.*, 31(5), 633–648,  
516 doi:10.1002/joc.2108, 2011.

517 Generoso, S., Bey, I., Labonne, M. and Bréon, F.-M.: Aerosol vertical distribution in dust outflow over the  
518 Atlantic: Comparisons between GEOS-Chem and Cloud-Aerosol Lidar and Infrared Pathfinder Satellite  
519 Observation (CALIPSO), *J. Geophys. Res.*, 113(D24), doi:10.1029/2008JD010154, 2008.

520 Ginoux, P., Chin, M., Tegen, I., Prospero, J. M., Holben, B., Dubovik, O. and Lin, S. J.: Sources and  
521 distributions of dust aerosols simulated with the GOCART model, *J Geophys Res-Atmos*, 106(D17),  
522 20255–20273, 2001.

523 Ginoux, P., Prospero, J. M., Gill, T. E., Hsu, N. C. and Zhao, M.: Global-scale attribution of anthropogenic  
524 and natural dust sources and their emission rates based on MODIS Deep Blue aerosol products, *Rev.*  
525 *Geophys.*, 50(3), doi:10.1029/2012RG000388, 2012.

526 Ginoux, P., Prospero, J. M., Torres, O. and Chin, M.: Long-term simulation of global dust distribution with  
527 the GOCART model: correlation with North Atlantic Oscillation, *Environ. Model. Softw.*, 19(2), 113–128,  
528 2004.

529 Haywood, J., Francis, P., Dubovik, O., Glew, M. and Holben, B.: Comparison of aerosol size distributions,  
530 radiative properties, and optical depths determined by aircraft observations and Sun photometers  
531 during SAFARI 2000, *J Geophys Res*, 108(D13), 2003.

532 Heald, C. L., Ridley, D. A., Kroll, J. H., Barrett, S. R. H., Cady-Pereira, K. E., Alvarado, M. J. and Holmes, C.  
533 D.: Beyond direct radiative forcing: the case for characterizing the direct radiative effect of aerosols,  
534 *Atmospheric Chem. Phys. Discuss.*, 13(12), 32925–32961, doi:10.5194/acpd-13-32925-2013, 2013.

535 Henze, D. K., Seinfeld, J. H., Ng, N. L., Kroll, J. H., Fu, T. M., Jacob, D. J. and Heald, C. L.: Global modeling  
536 of secondary organic aerosol formation from aromatic hydrocarbons: high- vs. low-yield pathways,  
537 *Atmospheric Chem. Phys.*, 8, 2405–2420, 2008.

538 Highwood, E. J.: Radiative properties and direct effect of Saharan dust measured by the C-130 aircraft  
539 during Saharan Dust Experiment (SHADE): 2. Terrestrial spectrum, *J. Geophys. Res.*, 108(D18),  
540 doi:10.1029/2002JD002552, 2003.

541 Hsu, N. C., Gautam, R., Sayer, A. M., Bettenhausen, C., Li, C., Jeong, M. J., Tsay, S.-C. and Holben, B. N.:  
542 Global and regional trends of aerosol optical depth over land and ocean using SeaWiFS measurements  
543 from 1997 to 2010, *Atmos Chem Phys*, 12(17), 8037–8053, doi:10.5194/acp-12-8037-2012, 2012.

544 Hsu, N. C., Herman, J. R. and Weaver, C.: Determination of radiative forcing of Saharan dust using  
545 combined TOMS and ERBE data, *J. Geophys. Res. Atmospheres*, 105(D16), 20649–20661,  
546 doi:10.1029/2000JD900150, 2000.

547 Huneeus, N., Schulz, M., Balkanski, Y., Griesfeller, J., Prospero, J., Kinne, S., Bauer, S., Boucher, O., Chin,  
548 M., Dentener, F., Diehl, T., Easter, R., Fillmore, D., Ghan, S., Ginoux, P., Grini, A., Horowitz, L., Koch, D.,  
549 Krol, M. C., Landing, W., Liu, X., Mahowald, N., Miller, R., Morcrette, J. J., Myhre, G., Penner, J., Perlwitz,  
550 J., Stier, P., Takemura, T. and Zender, C. S.: Global dust model intercomparison in AeroCom phase I,  
551 *Atmospheric Chem. Phys.*, 11(15), 7781–7816, 2011.

552 Hurrell, J. W.: Decadal Trends in the North Atlantic Oscillation: Regional Temperatures and Precipitation,  
553 *Science*, 269(5224), 676–679, doi:10.1126/science.269.5224.676, 1995.

554 Hwang, Y.-T., Frierson, D. M. W. and Kang, S. M.: Anthropogenic sulfate aerosol and the southward shift  
555 of tropical precipitation in the late 20th century, *Geophys. Res. Lett.*, 40(11), 2845–2850,  
556 doi:10.1002/grl.50502, 2013.

557 Jaegle, L., Quinn, P. K., Bates, T. S., Alexander, B. and Lin, J.-T.: Global distribution of sea salt aerosols:  
558 new constraints from in situ and remote sensing observations, *Atmos Chem Phys Discuss*, 10, 25687–  
559 25742, 2010.

560 Kaufman, Y. J., Koren, I., Remer, L. A., Tanre, D., Ginoux, P. and Fan, S.: Dust transport and deposition  
561 observed from the Terra-Moderate Resolution Imaging Spectroradiometer (MODIS) spacecraft over the  
562 Atlantic ocean, *J. Geophys. Res.-Atmospheres*, 110(D10), doi:10.1029/2003JD004436, 2005a.

563 Kaufman, Y., Koren, I., Remer, L. A., Rosenfeld, D. and Rudich, Y.: The effect of smoke, dust, and  
564 pollution aerosol on shallow cloud development over the Atlantic Ocean, *PNAS*, 102(32), 11207–11212,  
565 2005b.

566 Kim, D., Chin, M., Bian, H., Tan, Q., Brown, M. E., Zheng, T., You, R., Diehl, T., Ginoux, P. and Kucsera, T.:  
567 The effect of the dynamic surface bareness on dust source function, emission, and distribution, *J.*  
568 *Geophys. Res. Atmospheres*, 118(2), 871–886, doi:10.1029/2012JD017907, 2013.

569 Kopke, P., Hess, M., Schult, I. and Shettle, E. P.: Global aerosol data set, Max Planck Inst. fur Meteorol.,  
570 Hamburg, Germany., 1997.

571 Koren, I., Feingold, G. and Remer, L. A.: The invigoration of deep convective clouds over the Atlantic:  
572 aerosol effect, meteorology or retrieval artifact?, *Atmospheric Chem. Phys.*, 10(18), 8855–8872, 2010.

573 Koven, C. D. and Fung, I.: Identifying global dust source areas using high-resolution land surface form, *J*  
574 *Geophys Res-Atmos*, 113, 19, doi:D22204 10.1029/2008jd010195, 2008.



575 Liao, H., Henze, D. K., Seinfeld, J. H., Wu, S. L. and Mickley, L. J.: Biogenic secondary organic aerosol over  
576 the United States: Comparison of climatological simulations with observations, *J. Geophys. Res.-*  
577 *Atmospheres*, 112(D6), doi:10.1029/2006JD007813, 2007.

578 Mahowald, N. M., Engelstaedter, S., Luo, C., Sealy, A., Artaxo, P., Benitez-Nelson, C., Bonnet, S., Chen, Y.,  
579 Chuang, P. Y., Cohen, D. D. and others: Atmospheric Iron Deposition: Global Distribution, Variability, and  
580 Human Perturbations, *Annu. Rev. Mar. Sci.*, 1, 245–278, 2009.

581 Martin, R. V., Jacob, D. J., Yantosca, R. M., Chin, M. and Ginoux, P.: Global and regional decreases in  
582 tropospheric oxidants from photochemical effects of aerosols, *J. Geophys. Res.-Atmospheres*, 108(D3),  
583 doi:10.1029/2002JD002622, 2003.

584 Mbourou, G. N., Bertrand, J. J. and Nicholson, S. E.: The diurnal and seasonal cycles of wind-borne dust  
585 over Africa north of the equator, *J Appl Meteorol*, 36(7), 868–882, 1997.

586 McGee, D., Broecker, W. S. and Winckler, G.: Gustiness: The driver of glacial dustiness?, *Quat. Sci. Rev.*,  
587 29(17–18), 2340–2350, doi:10.1016/j.quascirev.2010.06.009, 2010.

588 McGee, D., deMenocal, P. B., Winckler, G., Stuut, J. B. W. and Bradtmiller, L. I.: The magnitude, timing  
589 and abruptness of changes in North African dust deposition over the last 20,000 yr, *Earth Planet. Sci.*  
590 *Lett.*, 371–372, 163–176, doi:10.1016/j.epsl.2013.03.054, 2013.

591 Miller, R. L., Tegen, I. and Perlwitz, J.: Surface radiative forcing by soil dust aerosols and the hydrologic  
592 cycle, *J Geophys Res*, 109(D04S03), 2004.

593 Mishchenko, M. I. and Geogdzhayev, I. V.: Satellite remote sensing reveals regional tropospheric aerosol  
594 trends, *Opt Express*, 15(12), 7423–7438, 2007.

595 Moulin, C., Lambert, C. E., Dulac, F. and Dayan, U.: Control of atmospheric export of dust from North  
596 Africa by the North Atlantic oscillation, *Nature*, 387(6634), 691–694, 1997.

597 Mulitza, S., Heslop, D., Pittauerova, D., Fischer, H. W., Meyer, I., Stuut, J.-B., Zabel, M., Mollenhauer, G.,  
598 Collins, J. A., Kuhnert, H. and Schulz, M.: Increase in African dust flux at the onset of commercial  
599 agriculture in the Sahel region, *Nature*, 466(7303), 226–228, doi:10.1038/nature09213, 2010.

600 Myhre, G., Samset, B. H., Schulz, M., Balkanski, Y., Bauer, S., Bernsten, T. K., Bian, H., Bellouin, N., Chin,  
601 M., Diehl, T., Easter, R. C., Feichter, J., Ghan, S. J., Hauglustaine, D., Iversen, T., Kinne, S., Kirkevåg, A.,  
602 Lamarque, J.-F., Lin, G., Liu, X., Lund, M. T., Luo, G., Ma, X., van Noije, T., Penner, J. E., Rasch, P. J., Ruiz,  
603 A., Seland, Ø., Skeie, R. B., Stier, P., Takemura, T., Tsigaridis, K., Wang, P., Wang, Z., Xu, L., Yu, H., Yu, F.,  
604 Yoon, J.-H., Zhang, K., Zhang, H. and Zhou, C.: Radiative forcing of the direct aerosol effect from  
605 AeroCom Phase II simulations, *Atmos Chem Phys*, 13(4), 1853–1877, doi:10.5194/acp-13-1853-2013,  
606 2013.

607 Nakamae, K. and Shiotani, M.: Interannual variability in Saharan dust over the North Atlantic Ocean and  
608 its relation to meteorological fields during northern winter, *Atmospheric Res.*, 122, 336–346,  
609 doi:10.1016/j.atmosres.2012.09.012, 2013.

610 Olsson, L., Eklundh, L. and Ardö, J.: A recent greening of the Sahel—trends, patterns and potential  
611 causes, *J. Arid Environ.*, 63(3), 556–566, doi:10.1016/j.jaridenv.2005.03.008, 2005.

612 Park, R. J., Jacob, D. J., Chin, M. and Martin, R. V.: Sources of carbonaceous aerosols over the United  
613 States and implications for natural visibility, *J. Geophys. Res.-Atmospheres*, 108(D12),  
614 doi:10.1029/2002JD003190, 2003.

615 Park, R. J., Jacob, D. J., Field, B. D., Yantosca, R. M. and Chin, M.: Natural and transboundary pollution  
616 influences on sulfate-nitrate-ammonium aerosols in the United States: Implications for policy, *J.*  
617 *Geophys. Res.-Atmospheres*, 109(D15), doi:10.1029/2003JD004473, 2004.

618 Prospero, J. M.: Long-term measurements of the transport of African mineral dust to the southeastern  
619 United States: Implications for regional air quality, *J Geophys Res-Atmos*, 104(D13), 15917–15927, 1999.

620 Prospero, J. M., Collard, F. X., Molinié, J. and Jeannot, A.: Characterizing the annual cycle of African dust  
621 transport to the Caribbean Basin and South America and its impact on air quality and the environment,  
622 *Glob. Biogeochem. Cycles*, Submitted.

623 Prospero, J. M., Ginoux, P., Torres, O., Nicholson, S. E. and Gill, T. E.: Environmental characterization of  
624 global sources of atmospheric soil dust identified with the Nimbus 7 Total Ozone Mapping Spectrometer  
625 (TOMS) absorbing aerosol product, *Rev Geophys*, 40(1), 31, doi:1002 10.1029/2000rg000095, 2002.

626 Prospero, J. M., Glaccum, R. A. and Nees, R. T.: Atmospheric Transport of Soil Dust from Africa to South-  
627 America, *Nature*, 289(5798), 570–572, 1981.

628 Prospero, J. M. and Lamb, P. J.: African droughts and dust transport to the Caribbean: Climate change  
629 implications, *Science*, 302(5647), 1024–1027, 2003.

630 Ridley, D. A., Heald, C. L. and Ford, B.: North African dust export and deposition: A satellite and model  
631 perspective, *J. Geophys. Res.*, 117(D2), doi:10.1029/2011JD016794, 2012.

632 Ridley, D. A., Heald, C. L., Pierce, J. R. and Evans, M. J.: Toward resolution-independent dust emissions in  
633 global models: Impacts on the seasonal and spatial distribution of dust, *Geophys. Res. Lett.*, 40(11),  
634 2873–2877, doi:10.1002/grl.50409, 2013.

635 Riemer, N., Doherty, O. M. and Hameed, S.: On the variability of African dust transport across the  
636 Atlantic, *Geophys. Res. Lett.*, 33(13), doi:10.1029/2006GL026163, 2006.

637 Rotstayn, L. D. and Lohmann, U.: Tropical rainfall trends and the indirect aerosol effect, *J. Clim.*, 15(15),  
638 2103–2116, 2002.

639 Savoie, D. L., Prospero, J. M. and Saltzman, E. S.: Non-sea-salt sulfate and nitrate in trade wind aerosols  
640 at Barbados: Evidence for long-range transport, *J. Geophys. Res. Atmospheres*, 94(D4), 5069–5080,  
641 doi:10.1029/JD094iD04p05069, 1989.

642 Schepanski, K., Tegen, I., Laurent, B., Heinold, B. and Macke, A.: A new Saharan dust source activation  
643 frequency map derived from MSG-SEVIRI IR-channels, *Geophys Res Lett*, 34(18), 5, doi:L18803  
644 10.1029/2007gl030168, 2007.

645 Schepanski, K., Tegen, I. and Macke, A.: Comparison of satellite based observations of Saharan dust  
646 source areas, *Remote Sens. Environ.*, 123, 90–97, doi:10.1016/j.rse.2012.03.019, 2012.

647 Shao, Y., Klose, M. and Wyrwoll, K.-H.: Recent global dust trend and connections to climate forcing, *J.*  
648 *Geophys. Res. Atmospheres*, 118(19), 11,107–11,118, doi:10.1002/jgrd.50836, 2013.

649 Sinyuk, A., Torres, O. and Dubovik, O.: Combined use of satellite and surface observations to infer the  
650 imaginary part of refractive index of Saharan dust, *Geophys. Res. Lett.*, 30(2), 2003.

651 Stephenson, D. B., Pavan, V. and Bojariu, R.: Is the North Atlantic Oscillation a random walk?, *Int. J.*  
652 *Climatol.*, 20(1), 1–18, doi:10.1002/(SICI)1097-0088(200001)20:1<1::AID-JOC456>3.0.CO;2-P, 2000.

653 Stier, P., Schutgens, N. A. J., Bellouin, N., Bian, H., Boucher, O., Chin, M., Ghan, S., Huneeus, N., Kinne, S.,  
654 Lin, G., Ma, X., Myhre, G., Penner, J. E., Randles, C. A., Samset, B., Schulz, M., Takemura, T., Yu, F., Yu, H.  
655 and Zhou, C.: Host model uncertainties in aerosol radiative forcing estimates: results from the AeroCom  
656 Prescribed intercomparison study, *Atmos Chem Phys*, 13(6), 3245–3270, doi:10.5194/acp-13-3245-2013,  
657 2013.

658 Stocker, T. F., Qin, D., Plattner, G. K., Tignor, M., Allen, S. K., Boschung, J., Nauels, A., Xia, Y., Bex, V. and  
659 Midgley, P. M.: IPCC, 2013: Summary for Policymakers. In: *Climate Change 2013: The Physical Science*  
660 *Basis.*, Cambridge University Press, Cambridge, United Kingdom and New York, NY, USA., 2013

661 Twohy, C. H., Kreidenweis, S. M., Eidhammer, T., Browell, E. V., Heymsfield, A. J., Bansemer, A. R.,  
662 Anderson, B. E., Chen, G., Ismail, S., DeMott, P. J. and Van Den Heever, S. C.: Saharan dust particles  
663 nucleate droplets in eastern Atlantic clouds, *Geophys. Res. Lett.*, 36(1), doi:10.1029/2008GL035846,  
664 2009.

665 Vautard, R., Cattiaux, J., Yiou, P., Thépaut, J.-N. and Ciais, P.: Northern Hemisphere atmospheric stilling  
666 partly attributed to an increase in surface roughness, *Nat. Geosci.*, 3(11), 756–761,  
667 doi:10.1038/ngeo979, 2010.

668 Viana, M., Querol, X., Alastuey, A., Cuevas, E. and Rodríguez, S.: Influence of African dust on the levels of  
669 atmospheric particulates in the Canary Islands air quality network, *Atmos. Environ.*, 36(38), 5861–5875,  
670 doi:10.1016/S1352-2310(02)00463-6, 2002.

671 Wang, C., Dong, S., Evan, A. T., Foltz, G. R. and Lee, S.-K.: Multidecadal Covariability of North Atlantic Sea  
672 Surface Temperature, African Dust, Sahel Rainfall, and Atlantic Hurricanes, *J. Clim.*, 25(15), 5404–5415,  
673 doi:10.1175/JCLI-D-11-00413.1, 2012.

674 Williams, K. D., Jones, A., Roberts, D. L., Senior, C. A. and Woodage, M. J.: The response of the climate  
675 system to the indirect effects of anthropogenic sulfate aerosol, *Clim. Dyn.*, 17(11), 845–856,  
676 doi:10.1007/s003820100150, 2001.

677 Yoshioka, M., Mahowald, N. M., Conley, A. J., Collins, W. D., Fillmore, D. W., Zender, C. S. and Coleman,  
678 D. B.: Impact of desert dust radiative forcing on Sahel precipitation: Relative importance of dust  
679 compared to sea surface temperature variations, vegetation changes, and greenhouse gas warming, *J.*  
680 *Clim.*, 20(8), 1445–1467, 2007.

681 Zender, C. S., Bian, H. S. and Newman, D.: Mineral Dust Entrainment and Deposition (DEAD) model:  
682 Description and 1990s dust climatology, *J. Geophys. Res.-Atmospheres*, 108(D14),  
683 doi:10.1029/2002JD002775, 2003.

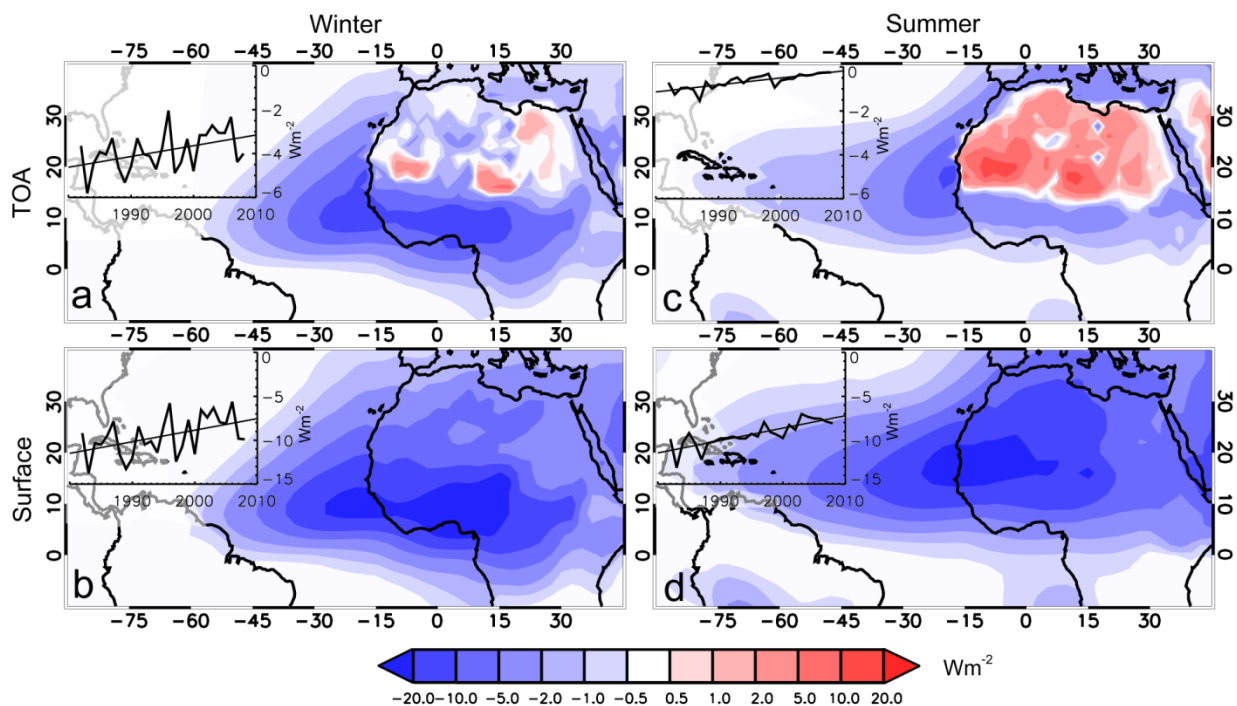
684 Zhang, R. and Delworth, T. L.: Impact of Atlantic multidecadal oscillations on India/Sahel rainfall and  
685 Atlantic hurricanes, *Geophys Res Lett*, 33(10.1029), 2006.

686 Zhao, T. X.-P., Laszlo, I., Guo, W., Heidinger, A., Cao, C., Jelenak, A., Tarpley, D. and Sullivan, J.: Study of  
687 long-term trend in aerosol optical thickness observed from operational AVHRR satellite instrument, J.  
688 *Geophys. Res. Atmospheres*, 113(D7), doi:10.1029/2007JD009061, 2008.

689

690 **Figure captions**

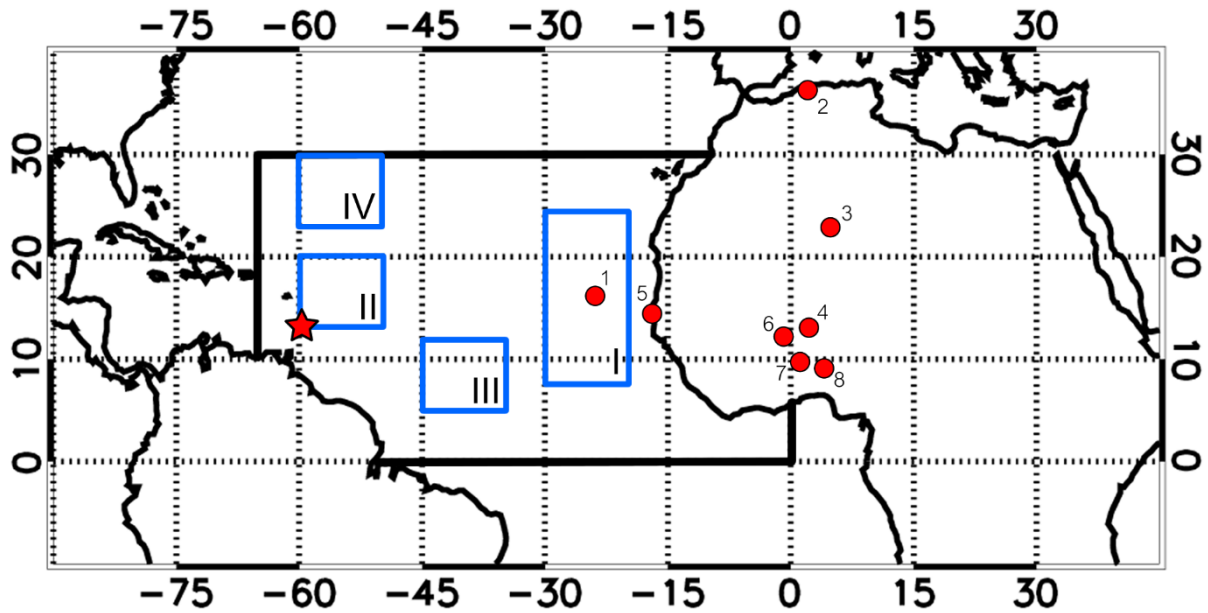
691



692

693 Figure 1 – Spatial maps of the average direct radiative effect of dust (DRE) at the surface and TOA  
694 are shown for both winter (left) and summer (right) seasons. The average is based on model  
695 output over the period 1982 – 2008. The inset shows the seasonal average DRE over the region  
696 0°N - 30°N, 50°W - 15°E. The thin black line indicates the trend over the simulation period.

697

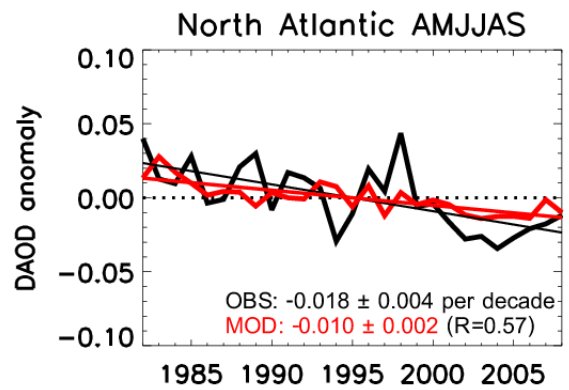
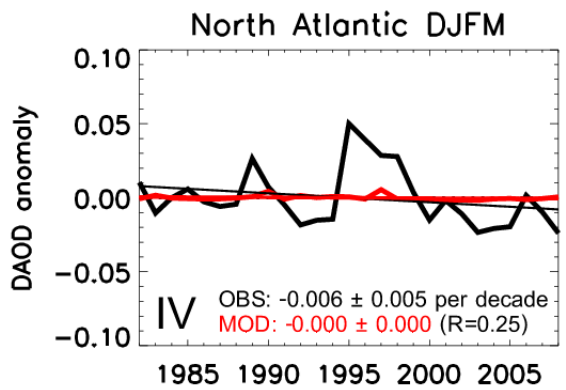
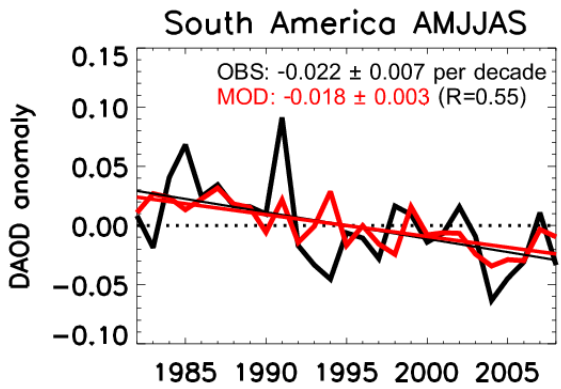
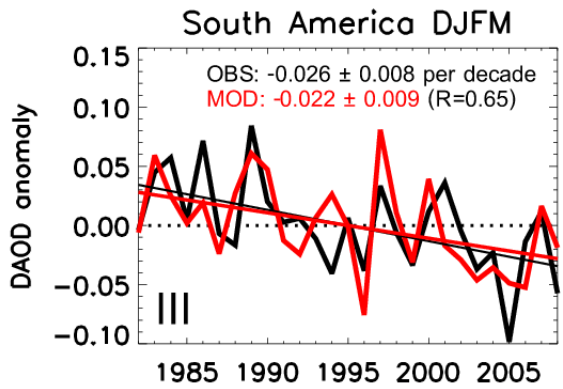
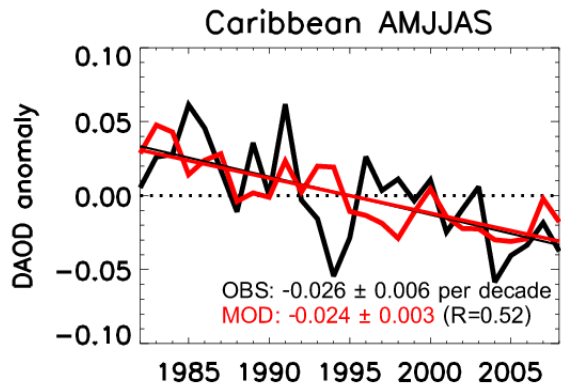
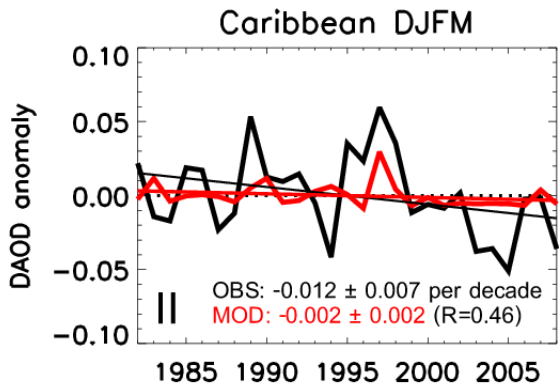
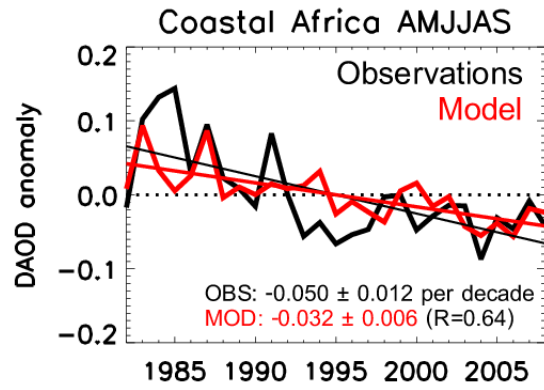
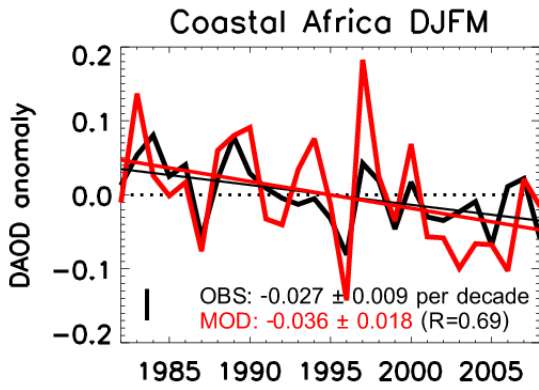


698

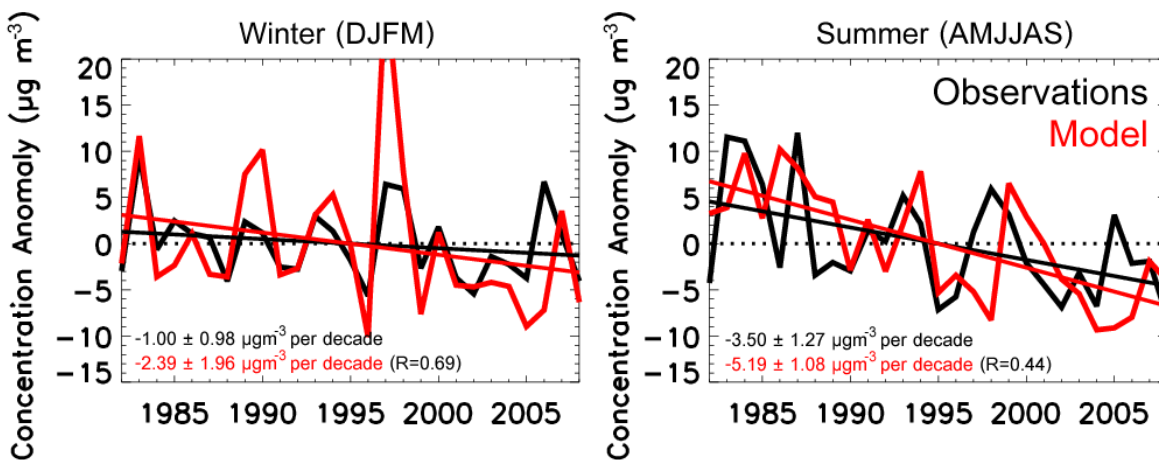
699 Figure 2 – The areas of interest for this study. The large black rectangle encloses the region  
 700 covered by the satellite-derived monthly dust AOD dataset and the blue rectangles (labelled with  
 701 roman numerals) are the regions within which model and satellite DAOD are compared. These  
 702 are referred to as (I) Coastal Africa, (II) Caribbean, (III) South America and (IV) North Atlantic.  
 703 Numbered circles indicate the location of AERONET sites used and the star shows the location of  
 704 the surface concentration measurements in Barbados.

705

706

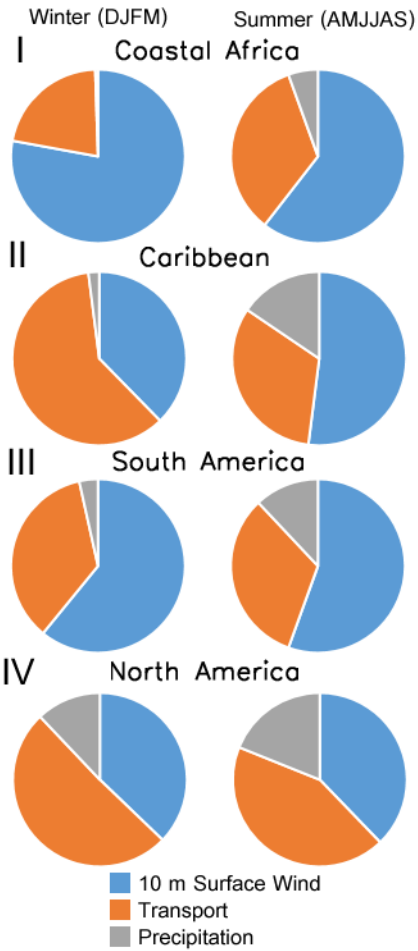


708 Figure 3 – Seasonal DAOD anomalies derived from AVHRR PATMOS-x (black) and from the model  
 709 (red) are displayed for four regions (roman numerals relate to the locations shown in Fig. 2).  
 710 Trend lines are plotted as solid lines and the trend and one standard deviation uncertainty shown  
 711 in each panel for the observations (OBS) and the model (MOD). The correlation (R) between  
 712 model and observations is shown in brackets.



713  
 714 Figure 4 – Seasonally-averaged surface concentrations anomalies from Barbados observations  
 715 (black) and from the model (red) are shown for winter and summer. Trend lines are plotted as  
 716 solid lines and the slope with one standard deviation indicated for each season. The correlation  
 717 (R) between the observations and model data is shown on each panel.

718



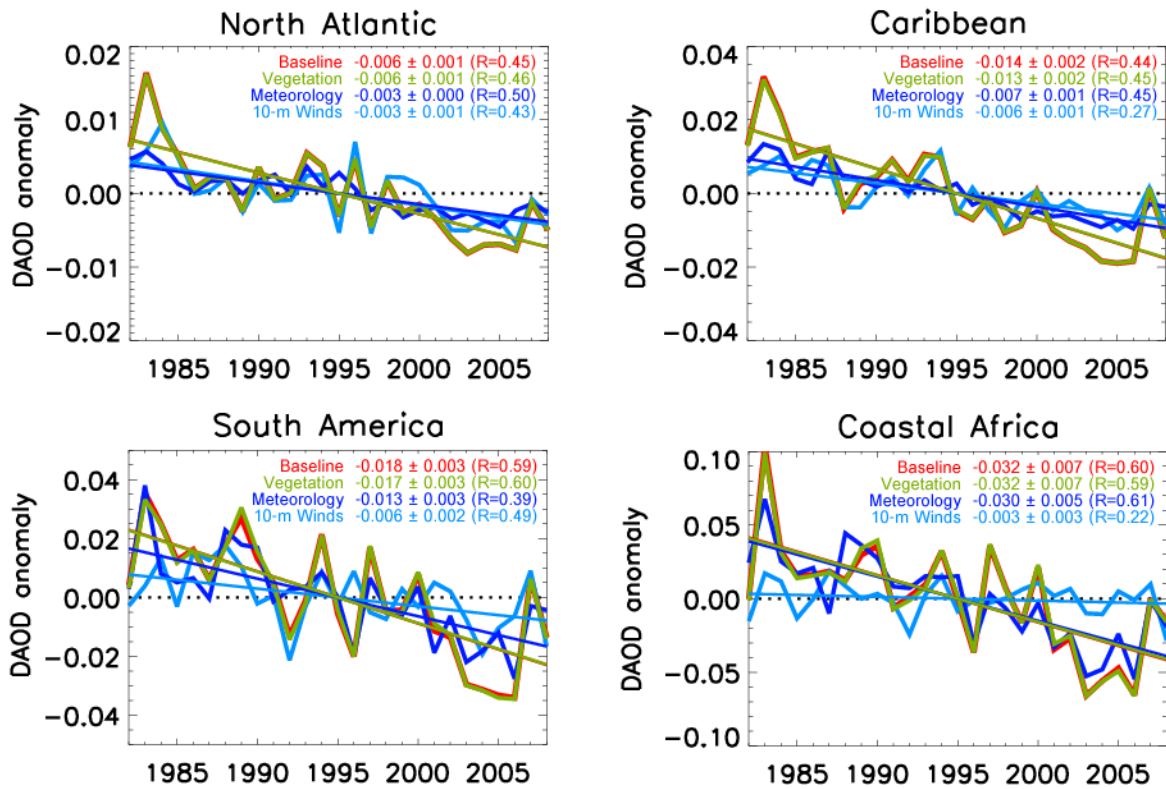
719

720 Figure 5 – Attribution of the interannual variability in dust is shown for the four regions in Fig. 2.

721 The approximate fraction of the variability owing to 10-m surface winds (blue), transport (orange)

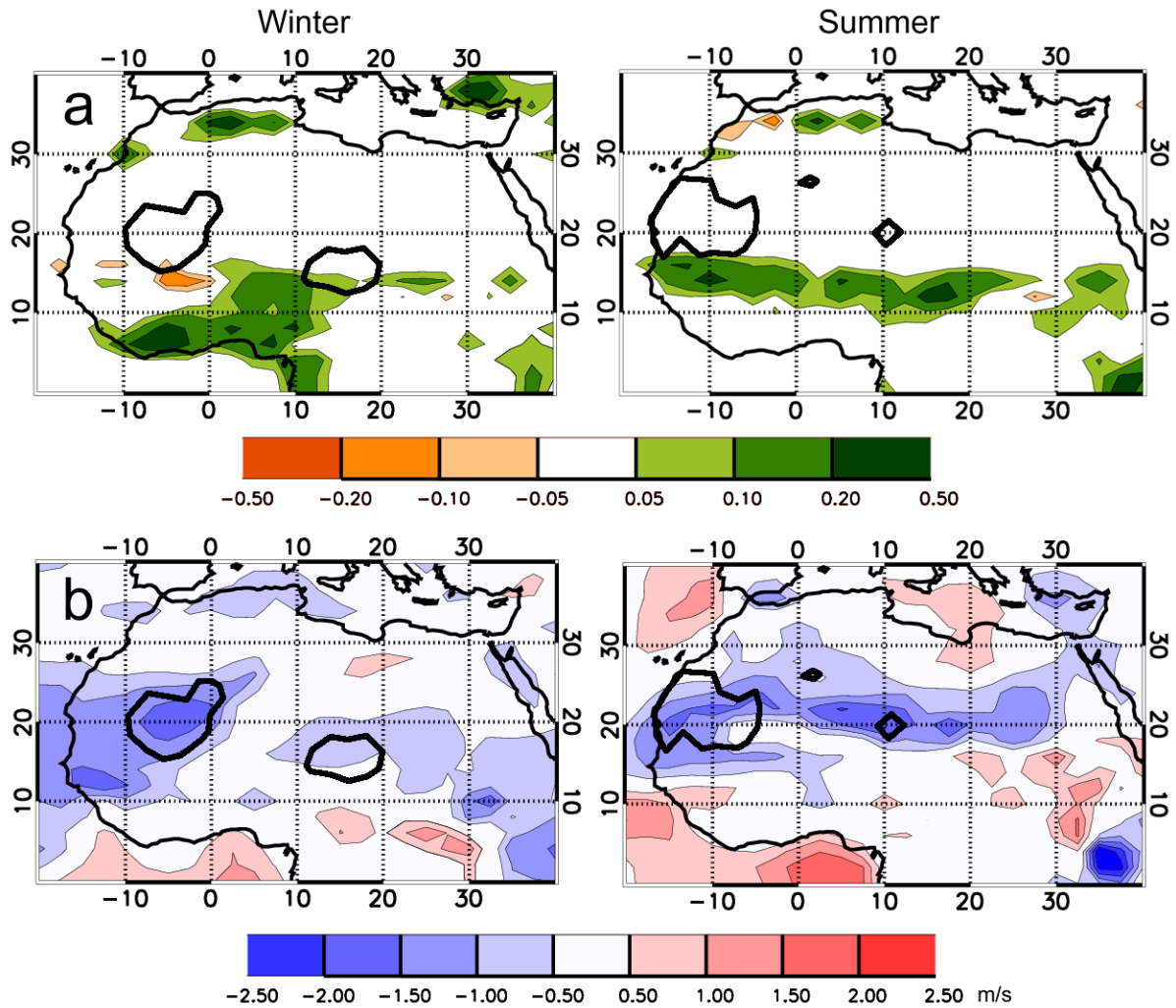
722 and precipitation (grey) is displayed for winter (left) and summer (right).





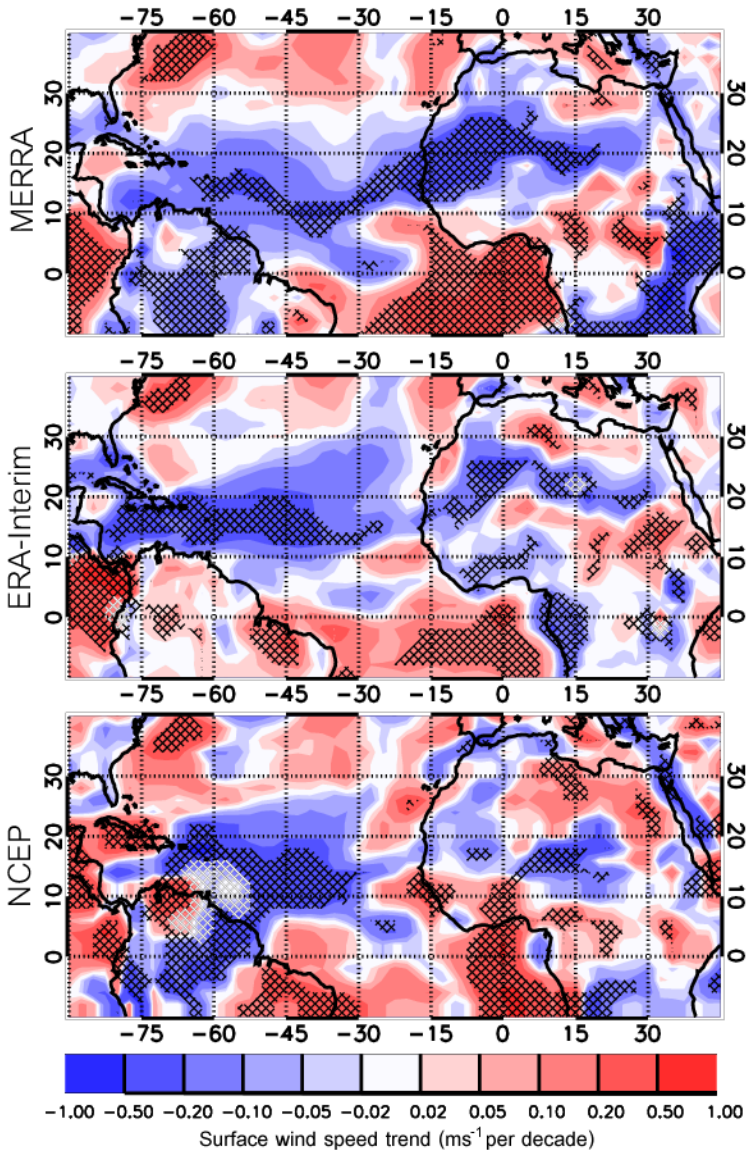
723

724 Figure 6 - Annual dust AOD (DAOD) anomalies are shown for the updated model (red, same as  
 725 the model in Fig. 2), with interannual variability in 10-m winds removed (light blue), with  
 726 interannual variability in all meteorology, except surface winds, removed (dark blue), and with  
 727 interannual variability in vegetation cover removed (green). Thin solid lines show the trends, and  
 728 the trend and one standard deviation uncertainty shown in each panel for the observations and  
 729 the model. The correlation between observed dust AOD and each version of the model is shown  
 730 in brackets. N.B. the red line is almost always obscured by the green line.



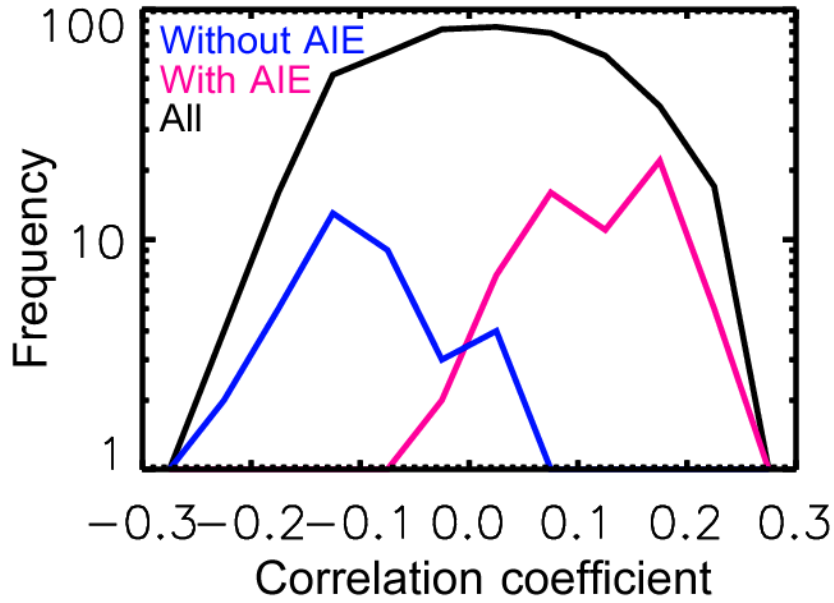
731

732 Figure 7 – The difference between 2002-2006 and 1982-1986 over North Africa is shown for (a)  
 733 fractional vegetation cover, represented by the decrease in bareness fraction, and (b) MERRA 10-  
 734 m wind speed. Black contours outline regions where emissions decrease by more than 0.5 Tg per  
 735 grid box.



736

737 Figure 8 – Spatial maps of the annual trend in surface winds between 1982 and 2008 based upon  
 738 the averaged winds from MERRA, ERA-Interim and NCEP/NCAR reanalysis. Regions with trends  
 739 that are significant at the 95% level are indicated with hashing.



740

741 Figure 9 – Histogram of the correlation between the spatial distribution of CMIP5 ensemble  
 742 surface wind trend and the reanalysis surface wind trend over 1982-2008. The histogram  
 743 represents 500 correlations, each based on the average surface winds of 3 randomly sampled  
 744 CMIP5 models (black). The blue histogram shows ensembles that only contain models with no  
 745 aerosol indirect effect (AIE) representation and the magenta distribution only those that do  
 746 contain a parameterization for the aerosol indirect effect.